

# Journal of Visualized Experiments

## Digital hybrid model preparation for virtual planning of reconstructive dentoalveolar surgical procedures --Manuscript Draft--

Article Type:	Methods Article - JoVE Produced Video
Manuscript Number:	JoVE62743R2
Full Title:	Digital hybrid model preparation for virtual planning of reconstructive dentoalveolar surgical procedures
Corresponding Author:	Daniel Palkovics Semmelweis University: Semmelweis Egyetem Budapest, Pest megye HUNGARY
Corresponding Author's Institution:	Semmelweis University: Semmelweis Egyetem
Corresponding Author E-Mail:	dpalkovics@gmail.com
Order of Authors:	Daniel Palkovics Eleonora Solyom Balint Molnar Csaba Pinter Peter Windisch
Additional Information:	
Question	Response
Please specify the section of the submitted manuscript.	Medicine
Please indicate whether this article will be Standard Access or Open Access.	Standard Access (\$1400)
Please indicate the <b>city, state/province, and country</b> where this article will be <b>filmed</b> . Please do not use abbreviations.	Budapest, Hungary
Please confirm that you have read and agree to the terms and conditions of the author license agreement that applies below:	I agree to the <a href="#">Author License Agreement</a>
Please provide any comments to the journal here.	
Please confirm that you have read and agree to the terms and conditions of the video release that applies below:	I agree to the <a href="#">Video Release</a>

**TITLE:**

Digital Hybrid Model Preparation for Virtual Planning of Reconstructive Dentoalveolar Surgical Procedures

**AUTHORS AND AFFILIATIONS:**

Daniel Palkovics<sup>1\*</sup>, Eleonora Solyom<sup>1</sup>, Balint Molnar<sup>1</sup>, Csaba Pinter<sup>2#</sup>, Peter Windisch<sup>1#</sup>

<sup>1</sup>Department of Periodontology, Semmelweis University, Hungary

<sup>2</sup>Empresa de Base Tecnológica Internacional de Canarias, S.L. (EBATINCA), Las Palmas de Gran Canaria, Spain

Email addresses of the authors:

Daniel Palkovics ([palkovics.daniel@dent.semmelweis-univ.hu](mailto:palkovics.daniel@dent.semmelweis-univ.hu))

Eleonora Solyom ([eleonorasolyom@gmail.com](mailto:eleonorasolyom@gmail.com))

Balint Molnar ([molbal81@gmail.com](mailto:molbal81@gmail.com))

Csaba Pinter ([pinter.csaba@gmail.com](mailto:pinter.csaba@gmail.com))

Peter Windisch ([peter.windisch@gmail.com](mailto:peter.windisch@gmail.com))

\*Email address of the corresponding author:

Daniel Palkovics ([palkovics.daniel@dent.semmelweis-univ.hu](mailto:palkovics.daniel@dent.semmelweis-univ.hu))

#Authors contributed equally to the preparation of the manuscript

**SUMMARY:**

A workflow for creating three-dimensional (3D) virtual hybrid models has been designed based on cone-beam computed tomography dataset and intraoral optical scans utilizing radiographic image segmentation methods and free-form surface modeling. Digital models are used for the virtual planning of reconstructive dentoalveolar surgical procedures.

**ABSTRACT:**

Virtual, hybrid three-dimensional (3D) model acquisition is presented in this article, utilizing the sequence of radiographic image segmentation, spatial registration, and free-form surface modeling. Firstly cone-beam computed tomography datasets were reconstructed with a semi-automatic segmentation method. Alveolar bone and teeth are separated into different segments, allowing 3D morphology, and localization of periodontal intrabony defects to be assessed. The severity, extent, and morphology of acute and chronic alveolar ridge defects are validated concerning adjacent teeth. On virtual complex tissue models, positions of dental implants can be planned in 3D. Utilizing spatial registration of IOS and CBCT data and subsequent free-form surface modeling, realistic 3D hybrid models can be acquired, visualizing alveolar bone, teeth, and soft tissues. With the superimposition of IOS and CBCT soft tissue, thickness above the edentulous ridge can be assessed about the underlying bone dimensions; therefore, flap design and surgical flap management can be determined, and occasional complications may be avoided.

**INTRODUCTION:**

Technological advancements in dentistry have enabled computer-aided treatment planning and simulation of surgical procedures and prosthetic rehabilitation. Two essential methods for 3D data acquisition in digital dentistry are: (1) cone-beam computed tomography (CBCT)<sup>1</sup> and (2) intraoral optical scanning (IOS)<sup>2</sup>. Digital information of all relevant anatomical structures (alveolar bone, teeth, soft tissues) can be acquired using these tools to plan reconstructive dentoalveolar surgical procedures.

Cone-beam technology was first introduced in 1996 by an Italian research group. Delivering significantly lower radiation dose and higher resolution (compared to conventional computed tomography), CBCT has quickly become the most frequently used 3D imaging modality in dentistry and oral surgery<sup>3</sup>. CBCT is often used to plan different surgical procedures (e.g., periodontal regenerative surgery, alveolar ridge augmentation, dental implant placement, orthognathic surgery)<sup>1</sup>. CBCT datasets are viewed and can be processed in radiographic imaging software that provides 2D images, and 3D renders—however, most imaging software use threshold-based algorithms for 3D image reconstruction. Thresholding methods set the upper and lower bounds of a voxel grey value interval. Voxels that fall in between these bounds will be rendered in 3D. This method allows speedy model acquisition; however, since the algorithm cannot differentiate anatomical structures from metal artifacts and scattering, the 3D renders are highly inaccurate and have very little diagnostic value<sup>4,5</sup>. For the reasons mentioned above, many fields within dentistry still rely on conventional 2D radiographs (intraoral radiographs, panoramic X-ray) or the 2D images of CBCT datasets<sup>5</sup>. Our research group presented a semi-automatic image segmentation method in a recently published article, using open-source radiographic image processing software<sup>6</sup> wherein anatomically based 3D reconstruction of CBCT datasets is performed<sup>7</sup>. With the help of this method, anatomical structures were differentiated from metal artifacts, and, more importantly, alveolar bone and teeth could be separated. Therefore, a realistic virtual model of hard tissues could be acquired. 3D models were used to evaluate intrabony periodontal defects and for treatment planning before regenerative periodontal surgeries.

Intraoral optical surface scanners provide digital information on clinical conditions (clinical crown of the teeth and soft tissues). The original intended purpose of these devices was to directly acquire digital models of patients for the planning and fabrication of dental prostheses with computer-aided design (CAD) and computer-aided manufacturing (CAM) technologies<sup>8</sup>. However, due to the wide range of applications, their use was quickly implemented in other fields of dentistry. Maxillo-facial surgeons combine IOS and CBCT into a hybrid setup that can be utilized for virtual osteotomy and digital planning of orthognathic surgeries<sup>9,10</sup>. Dental implantology is probably the field that uses digital planning and guided execution most commonly. Navigated surgery eliminates most complications related to implant mispositioning. The combination of CBCT datasets and stereolithography (.stl) files of IOS is routinely used to plan the guided implant placement and the fabrication of static implant drilling guides<sup>11,12</sup>. Intraoral scans superimposed over CBCT datasets have also been used to prepare esthetic crown lengthening<sup>13</sup>; however, soft tissues were superimposed only over CBCT datasets reconstructed with thresholding algorithms. Yet, to perform accurate 3D virtual planning of regenerative-reconstructive surgical interventions and dental implant placement, realistic 3D hybrid models of patients must be composed of CBCT

and IOS data.

Hence, this article aims to present a step-by-step method to acquire realistic hybrid digital models for virtual surgical planning before reconstructive dentoalveolar surgical interventions.

#### **PROTOCOL:**

This study was conducted in complete accordance with the Declaration of Helsinki. Before manuscript preparation, written informed consent was provided and signed by the patient. The patient granted permission for data usage for the demonstration of the protocol.

### **1. Radiographic image processing**

#### **1.1. Load DICOM files into the software**

##### **1.1.1. Download the newest version of the medical imaging software and open it.**

NOTE: After opening the software, the home screen will appear.

##### **1.1.2. Click **Load DICOM Data** on the sidebar.**

NOTE: The DICOM database will pop up, showing the previously loaded DICOM datasets.

##### **1.1.2.1 Click **Import DICOM files** in the DICOM database, select the DICOM dataset in the destination folder and click **Import**.**

NOTE: The newly added DICOM dataset will appear in the list of studies.

##### **1.1.3. Select the study and click **Load** at the bottom of the window.**

NOTE: The DICOM dataset will be opened, and four views (coronal, axial, sagittal, and 3D) of the loaded data will be visible. Nodes are listed on the left-hand side. Theoretically, the described method can be performed on any CT or CBCT regardless of image quality (voxel size, artifacts). However, the segmentation process of higher-quality CBCT/CT scans is more straightforward, and higher-quality 3D models can be acquired. A shown CBCT scan was taken with the following parameters: voxel size: 150  $\mu$ m, anode voltage: 84 kV, tube current: 40 mA, Field-of-view: 8 x 5 cm. The process can be stopped at any stage; make sure to save the scene before exiting. To save, click the save icon on the left-hand side of the toolbar and save it as a “medical record bundle” (.mrb) by clicking on the box icon in the “save scene” window.

#### **1.2. Volume rendering and cropping volume**

##### **1.2.1. Crop the area of interest (upper or lower jaw) to reduce the file size and rendering time. Click the **Modules** bar visible on the left-hand side of the toolbar to view a scroll-down window showing frequently used modules.**

1.2.2. Select the **Volume Rendering** module from the dropdown window. To make volume rendering visible, click the **eye** icon next to the “Volumes” bar.

1.2.3. Select the desired preset to view the volume render and move the “Shift” slider until the hard tissues can be viewed clearly.

NOTE: For CBCT scans, the CT-Bone preset is recommended.

1.2.4. Check the box next to “Enable” and click the **eye** icon next to “Display ROI” in the “Crop” section to make the ROI (Region of interest) visible.

NOTE: A wireframe box around the dataset in all 2D views and the 3D view will appear. By dragging the sides of the box, the volume will be cropped to the desired area.

1.2.5. Access the “Crop Volume” module to finalize cropping. Select the original dataset as the input volume.

NOTE: Input ROI is automatically set to ROI that was previously created.

1.2.6. Select **Create new volume** from the “Output volume” dropdown bar to create a new output volume. Uncheck **Interpolated cropping** in the advanced settings section and click **Apply**.

NOTE: When returning to the “Data module,” the new cropped volume will appear as a new node.

### 1.3. Segmentation of CBCT dataset

#### 1.3.1. Access the **Segment Editor** module for segmentation.

NOTE: Segmentation is when 3D reconstructions of anatomical structures are generated based on the CBCT dataset to allow more accessible analysis.

1.3.2. Select the previously created cropped volume as the **Master Volume** of the active segmentation. Click **+Add** to add, and **-Remove** to remove segments. Rename them according to the anatomical structure they will represent.

NOTE: Alveolar bone and all teeth will be separate segments within the segmentation

1.3.3. Start with the segmentation of the alveolar bone. From the list of effects, select **Level Tracing**, a semi-automatic tool that outlines the region where pixels have the same background value as the selected pixel.

1.3.4. Drag the mouse to the perimeter of the bone on one of the 2D views for a yellow line to

appear around the selected area and press the **left mouse button** to generate the segment on the selected slice of the dataset.

NOTE: Segmentation can be done in any of the 2D views; however, sagittal and axial orientations work the best.

1.3.5. Use the **Paint** and **Erase** hand tools to modify the segment and correct mistakes if the “Level Tracing” tool did not outline the entire section of the bone or if artifacts present on the slice were also included.

[Place **Figure 1** here]

NOTE: Using number keys to allow fast switching between tools.

1.3.6. Exclude both teeth and implants from the bone segment. Outline teeth and implants using the **Erase** tool and delete all highlighted pixels representing them.

1.3.7. Repeat the same process on every 5<sup>th</sup> slice of the dataset in the selected orientation.

NOTE: Click **Show 3D** to view the segmentation in three dimensions. Set the smoothing factor slider to 0.00.

1.3.8. Compute the missing segments upon completion of this phase—select **Fill between slices** from the effects list.

NOTE: This tool calculates the missing segments based on those created previously using a morphological contour interpolation algorithm.

1.3.9. Click **Initialize** to activate contour interpolation, and if the results are satisfactory, click **Apply**. Scroll through the dataset upon completion to check and correct occasional mistakes.

[Place **Figure 2** here]

NOTE: Make sure that only the segment is visible on which the interpolation is applied. The visibility of the segments can be toggled in the segments list.

1.3.10. Make segment boundaries smoother by removing protrusions using the **Smoothing** effect. Select **Median** as the smoothing method and set the “Kernel size” to **5 x 5 x 5** pixels by adjusting the mm value in the bracket and clicking **Apply**.

1.3.11. Repeat the same steps for the segmentation of teeth once the segmentation of alveolar bone is completed.

[Place **Figure 3** here]

1.3.12. Set the “Modify other segments” bar to **Allow overlap** before tooth segmentation so that the newly created segments will not overwrite the previously created ones.

#### 1.4. Spatial registration of CBCT dataset and IOS

NOTE: Spatial registration is necessary because the coordinate systems for the CBCT dataset and the IOS are different.

1.4.1. Select **Extension Manager** From the “View” menu bar and click **Install Extensions**. Type **IGT** into the search bar in the right-hand corner, install the **SlicerIGT** extension and restart the program.

1.4.2. Load the previously saved .mrb file of the scene by clicking the **Data** icon and **Choose file(s) to add**.

1.4.3. Import the .stl file of IOS by clicking the **Data** icon in the upper left corner. In the “Add data into the scene” pop-up window, click **Choose file(s) to add**, go to the destination folder, select the .stl file of the IOS, and click **Open**.

1.4.4. Add the .stl file of the intraoral scan as segmentation by selecting **Segmentation** from the dropdown bar.

NOTE: The installed “IGT” module will now appear in the “Modules” dropdown menu.

1.4.5. Move the cursor over the module, and in the sidebar that appears, select **Fiducial Registration Wizard**.

1.4.6. Select **Create new Markups Fiducial** from the dropdown bar in both the “From fiducials” and the “To fiducials” sections.

NOTE: The software will automatically name the two lists “From” and “To.” The “From” list represents the moving volume, which in this case will be the IOS. The “To” list represents the fixed volume, which will be the CBCT dataset.

1.4.7. Place marker points on well-defined anatomical landmarks on the IOS using the “Place a markup point” icon next to the dropdown bar in the “From” section. Markup points will be numbered in order of placement.

NOTE: Place at least 6 points on the cusps and incisal edges of teeth.

1.4.8. Place markers in the same position to create the “To” list and in the same order on the CBCT dataset. Markup points with the same number must represent the same anatomical landmark.

1.4.9. Create a transformation by selecting **Create new LinearTransform** from the dropdown menu in the “Registration result transform” section of the sidebar after the two lists are ready.

1.4.10. Access the “Transforms” module and select the previously created transformation as the **Active transform**. In the “Apply transform” section, move the IOS segmentation and the “From” markups list from the “Transformable” box to the “Transformed” box to superimpose the IOS over the CBCT dataset.

[Place **Figure 4** here]

NOTE: If necessary, the accuracy of the transformation can be improved by moving the markup points or by adding additional points.

2. Export models as .stl files for free-form surface modeling

2.1. Export the matched hard- and soft-tissue models for further surface modeling after segmentation and spatial registration.

2.2. Go to the **Segmentations** module and select the segmentation with the alveolar bone and teeth models as the active segmentation. Scroll down to the “Export to files” section, choose the destination folder, and select **STL** as the file format.

2.3. Uncheck the **Merge into single file** box, set the Coordinate system to **RAS**, and click **Export**.

2.4. Repeat the same process for the IOS, visible as a separate segmentation, save the scene, and close the imaging software.

3. Free-form surface modeling

3.1. Surface smoothing

3.1.1. Open the CAD software, and on the home screen, click **Import**. Select the .stl models that were previously exported from the DICOM image processing software.

NOTE: Even though smoothing was performed previously, the surface of the models reconstructed from the CBCT dataset will still appear pixelated, so further surface smoothing is necessary.

3.1.2. Go to **Sculpt** in the menu bar, and from the brush inventory, select **Adaptive reduce**.

NOTE: Brush size and strength must be adjusted, depending on the amount of smoothing.



### 3.2. Separate crown of the teeth from the IOS

NOTE: Crowns of teeth are depicted more accurately on the IOS than on segmented models; therefore, crowns of the segmented teeth models must be replaced with crowns from the IOS.

3.2.1. Click **Select** in the sidebar and select **Brush** as the selection tool. Use **Unwrap brush** brush mode and adjust the size of the brush. Using the brush, select the crown of each tooth until the marginal gingiva on the IOS.

NOTE: Selected surfaces are indicated with an orange color.

3.2.2. Move the cursor to **Modify** in the sidebar and select **Smooth Boundary**. Click **Apply** if the results are satisfactory.

NOTE: Now, the boundary of the selection precisely follows the marginal gingiva.

3.2.3. Go to **Edit** in the **Select** sidebar and click **Separate** to create an individual object from the selected area.

3.2.4. Repeat the same process for all teeth.

3.2.5. Go to **Analysis** in the menu bar and select **Inspect**.

NOTE: The program will indicate errors in the models. Holes are marked with a blue color.

3.2.6. Select **Flat fill** as the “Hole fill mode” and click **Auto repair all** to create closed models from the IOS model and the separated teeth models. Go to **Sculpt** and smooth the edges of the filled hole using **Shrinksmooth** brush.

3.2.7. Repeat the process for all tooth crowns and the rest of the IOS.

### 3.3. Merge crowns of the teeth with the segmented tooth models.

NOTE: If spatial registration was correctly done, the positions of the crowns of teeth on the IOS and the crowns of segmented teeth should match.

3.3.1. Use the **Shrinksmooth** brush on the segmented tooth model until they are completely cover by the tooth crowns separated from the IOS.

NOTE: Due to imperfections in both the segmentation and the IOS, the crowns don't always overlap completely.

3.3.2. Select both the separated crown and the segmented model of the same tooth in the **Object Browser**. In the sidebar that appears, select **Boolean union**, and click **Accept**.

NOTE: Now, the crown of the segmented tooth model is replaced by the crown separated from the IOS.

3.3.3. Use **Shrinksmooth** to smooth the transition.

3.4. Subtractions and model composition

3.4.1. Subtract the bone model from the soft-tissue model to represent the clinical situation realistically.

NOTE: The original IOS without teeth became the model of the soft tissues.

3.4.2. Select both bone and soft-tissue models in the **Object Browser** and select **Boolean Difference**.

3.4.3. Smooth transitions with the **Shrinksmooth** brush and remove protrusions from the bottom side of the soft-tissue model.

3.4.4. Subtract teeth from the soft-tissue model using the same process and smooth transitions.

3.5. Color models

3.5.1. Color the surfaces of the models to give a more realistic look since the model is complete now with the teeth, soft tissues, and alveolar bone being separated from one another, representing the clinical situation in 3D.

3.5.2. Select **Sculpt** from the sidebar and switch the little slider from **Volume** to **Surface**.

3.5.3. Select **PaintVertex** from the brush inventory and select the desired color using the color wheel in the **Color** section of the sidebar. Color the surface of each model (e.g., bone: brown, soft tissue: pink, teeth: white)

[Place **Animated Figure 1** here]

## REPRESENTATIVE RESULTS:

Virtual allowing three-dimensional (3D) models can be generated using radiographic image segmentation, spatial registration, and free-form modeling. The models digitally depict the clinical situation, making three-dimensional planning of various surgical interventions possible. With separate segmentation of bone and teeth, the boundary between the two anatomical structures is visible, 3D morphology and localization of periodontal intrabony defects are to be assessed. The severity, extent, and morphology of acute and chronic alveolar ridge defects can be evaluated concerning adjacent teeth. Various semi-automatic segmentation tools (**Figure 1**)

(Figure 2) (e.g., edge detection tools, morphological contour interpolation algorithms) found in medical image processing software inventories reduce the duration of segmentation (Figure 3). However, due to similarities in voxel intensity values of teeth and alveolar bone, separation of the two has to be done by hand, which can be time-consuming. The segmentation process is also hindered by artifacts present on CBCT scans.

Superimposition of IOS and subsequent CAD modeling allows for viewing the clinical situation in three dimensions. Teeth are separated from soft tissues on the model of the IOS (Figure 4). 3D models of teeth are combined from CBCT, and IOS data since tooth crowns on the IOS more accurately represent the clinical situation, whereas artifacts and scatter on the CBCT scan are compromised. With the superimposition of IOS and CBCT soft tissue, thickness above the edentulous ridge can be assessed about the underlying bone dimensions; therefore, flap design and surgical flap management can be determined, and occasional complications may be avoided (Animated Figure1).

#### FIGURE LEGENDS:

**Figure 1: Application of “Level Tracing” semi-automatic segmentation tool in sagittal orientation. (A)** Outlining the region of pixels with the same background value with a yellow line. **(B)** Results of “Level Tracing” and subsequent manual segmentation. **(C)** Refinement of semi-automatic segmentation with the help of manual tools (paint, erase).

**Figure 2: Morphological contour interpolation with “Fill Between Slices,” light green areas indicating the automatically reconstructed part of the segment. (A)** Axial view. **(B)** Sagittal view. **(C)** Coronal view.

**Figure 3: Finished segmentation, the brown segment representing bone and the blue segment representing teeth. (A)** Axial view. **(B)** Sagittal view. **(C)** Coronal view. **(D)** The 3D model is generated automatically from the segments created previously.

**Figure 4: Spatial registration of IOS by placing fiducial markers on well-defined anatomical landmarks.**

**Animated Figure 1: Animation of the final, colored model, ready for virtual surgical planning.**

#### DISCUSSION:

With the presented protocol, periodontal and alveolar defect morphologies can be visualized in three dimensions (3D), providing a more accurate depiction of the clinical situation than can be achieved by 2D diagnostic methods and 3D models generated with thresholding algorithms. The protocol can be divided into three major phases: (1) semi-automatic segmentation of CBCT datasets, (2) spatial registration of CBCT and IOS, and (3) free-form surface modeling. Technically, segmentation can be performed on any three-dimensional radiographic image; however, it is more challenging to reconstruct low-quality datasets. Therefore, a smaller voxel size ( $\sim 120 \mu\text{m}$ ), tube current (12 mA), and anode voltage (80 kV) are recommended<sup>14</sup>. Due to a large amount of

scatter generated at the occlusal plane, interocclusal space should be preserved during CBCT imaging.

Specific steps of the semi-automatic segmentation process are automated, but some actions still require segmentation by hand, which lengthens the duration of the process. For reducing the timeframe of the segmentation, artificial intelligence-based (AI) convolution neural networks have been developed for fast, automatic segmentation of tooth and bone<sup>15,16</sup>. In machine learning, convolution neural networks for image analysis are developed with representation learning on a sample database, in which features on the images must be similar. However, due to the morphological diversity of periodontal and alveolar defects, differences in radiographic density, and lack of corticalization at pathologic areas, results of AI-based segmentation may be compromised. Machine learning algorithms work reliably in physiological tissue conditions.

Spatial registration of IOS over CBCT data has been utilized to plan maxillofacial surgeries<sup>9,10</sup>, implant placement<sup>11,12</sup> and periodontal surgeries<sup>7,13</sup>, although free-form modeling was not applied. With a series of Boolean operations, realistic hybrid models can be acquired, and surgical interventions can be simulated virtually. Digital renders can also be manufactured with 3D printing technologies to produce study models before surgery.

The advantage of the present method is that the entire process can be done using free, open-source software. However, it has a learning curve, and users must familiarize themselves with radiographic image processing and free-form CAD modeling. The most significant drawback of the method is the relatively long duration and repetitive nature of the process. Therefore, improvements are needed to automate and simplify specific steps in the workflow to shorten the timeframe.

Three-dimensional design and CAD modeling have been utilized in the planning of various reconstructive surgical interventions. In periodontal diagnostics, 3D models generated with CBCT image reconstruction were being used for the preoperative assessment of intrabony defect morphologies and surgical treatment planning<sup>7</sup>. CAD/CAM allogenic bone blocks were utilized for onlay grafting<sup>17</sup>. Individually fabricated titanium meshes<sup>18</sup> were applied as barrier membranes in guided bone regeneration; however, soft-tissue models were not included in the planning process. Guided implant placement is routinely performed in daily dental practice with high reliability<sup>19</sup>.

Nevertheless, the majority of implant guide software utilizes thresholding algorithms for the 3D reconstruction of complex tissues. Even though planning is theoretically possible on 3D renders, due to the low quality of the bone models, implant positions are mainly planned on the axial, sagittal, and coronal 2D views of the CBCT dataset. To add another layer of reality, digital face scan acquired with free mobile applications could be added in the future.

With the sequence of radiographic image segmentation, spatial registration, and free-form surface modeling, realistic patient-specific virtual models can be acquired to plan reconstructive surgical interventions. With the virtual 3D depiction of bone, teeth, and soft tissues, each step of

the surgical intervention (i.e., incision, flap preparation, regenerative strategy, flap closure) can be predesigned and simulated virtually.

#### **DISCLOSURES:**

The authors declare no conflict of interest.

#### **ACKNOWLEDGMENTS:**

None

#### **REFERENCES:**

1. Jacobs, R., Salmon, B., Codari, M., Hassan, B., Bornstein, M. Cone beam computed tomography in implant dentistry: recommendations for clinical use. *BMC Oral Health*. **18** (1), 88 (2018).
2. Mangano, F., Gandolfi, A., Luongo, G., Logozzo, S. Intraoral scanners in dentistry: a review of the current literature. *BMC Oral Health*. **17** (1), 149 (2017).
3. Pauwels, R., Araki, K., Siewerdsen, J. H., Thongvigitmanee, S. S. Technical aspects of dental CBCT: state of the art. *Dentomaxillofacial Radiology*. **44** (1), 20140224 (2015).
4. Queiroz, P. M., Santaella, G. M., Groppo, F. C., Freitas, D. Q. Metal artifact production and reduction in CBCT with different numbers of basis images. *Imaging Science in Dentistry*. **48** (1), 41–44 (2018).
5. Scarfe, W. C., Azevedo, B., Pinheiro, L. R., Priaminiarti, M., Sales, M. A. O. The emerging role of maxillofacial radiology in the diagnosis and management of patients with complex periodontitis. *Periodontology 2000*. **74** (1), 116–139 (2017).
6. Fedorov, A. et al. 3D Slicer as an image computing platform for the Quantitative Imaging Network. *Magnetic Resonance Imaging*. **30** (9), 1323–1341 (2012).
7. Palkovics, D., Mangano, F. G., Nagy, K., Windisch, P. Digital three-dimensional visualization of intrabony periodontal defects for regenerative surgical treatment planning. *BMC Oral Health*. **20** (1), 351 (2020).
8. Papadiochou, S., Pissiotis, A. L. Marginal adaptation and CAD-CAM technology: A systematic review of restorative material and fabrication techniques. *Journal of Prosthetic Dentistry*. **119** (4), 545–551 (2018).
9. Xia J. J. et al., Algorithm for planning a double-jaw orthognathic surgery using a computer-aided surgical simulation (CASS) protocol. Part 1: planning sequence. *International Journal of Oral Maxillofacial Surgery*. **44** (12), 1431–40 (2015).
10. Xia, J. J. et al. Algorithm for planning a double-jaw orthognathic surgery using a computer-aided surgical simulation (CASS) protocol. Part 2: three-dimensional cephalometry. *International Journal of Oral Maxillofacial Surgery*. **44** (12), 1441–50 (2015).
11. Lee, C. Y., Ganz, S. D., Wong, N., Suzuki, J. B. Use of cone beam computed tomography and a laser intraoral scanner in virtual dental implant surgery: part 1. *Implant Dentistry*. **21** (4), 265–71 (2012).
12. Ganz, S. D. Three-dimensional imaging and guided surgery for dental implants. *Dental Clinics of North America*. **59** (2), 265–90 (2015).
13. Güth, J. F., Kauling, A. E. C., Schweiger, J., Kühnisch, J., Stimmelmayer, M. Virtual simulation of periodontal surgery including presurgical CAD/CAM fabrication of tooth-colored removable

- 529 splints on the basis of CBCT Data: A case report. *The International Journal of Periodontics &*  
530 *Restorative Dentistry*. **37** (6), e310-e320 (2017).
- 531 14. Pauwels, R. et al. Effective radiation dose and eye lens dose in dental cone beam CT:  
532 effect of field of view and angle of rotation. *The British Journal of Radiology*. **87** (1042), 20130654  
533 (2014).
- 534 15. Li, Q., Chen, K., Han, L., Zhuang, Y., Li, J., Lin, J. Automatic tooth roots segmentation of  
535 cone beam computed tomography image sequences using U-net and RNN. *Journal of X-ray*  
536 *Science and Technology*. **28** (5), 905-922 (2020).
- 537 16. Lahoud, P. et al. Artificial intelligence for fast and accurate 3D tooth segmentation on  
538 CBCT. *Journal of Endodontics*. **47** (5), 827-835 (2021).
- 539 17. Blume, O., Donkiewicz, P., Back, M., Born, T. Bilateral maxillary augmentation using  
540 CAD/CAM manufactured allogenic bone blocks for restoration of congenitally missing teeth: A  
541 case report. *Journal of Esthetic and Restorative Dentistry*. **31** (3), 171–178 (2019).
- 542 18. Hartmann, A., Seiler, M. Minimizing risk of customized titanium mesh exposures - a  
543 retrospective analysis. *BMC Oral Health*. **20** (1), 36 (2020).
- 544 19. Varga, E. Jr. et al. Guidance means accuracy: A randomized clinical trial on freehand versus  
545 guided dental implantation. *Clinical Oral Implants Research*. **31** (5), 417–430 (2020).

Figure 1



Figure 2

[Click here to access/download;Figure;Figure2.psd](#)

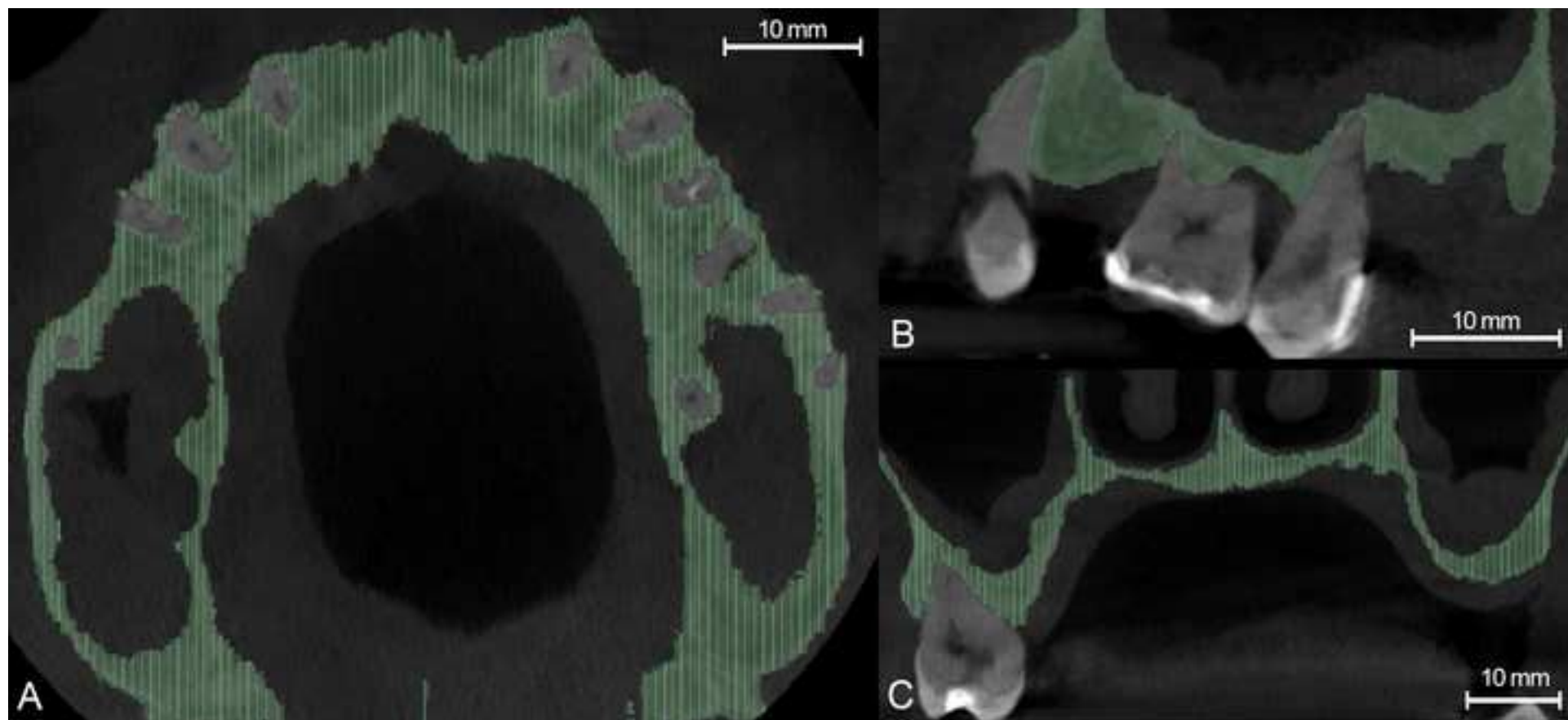




Figure 3

[Click here to access/download;Figure;Figure3.psd](#)

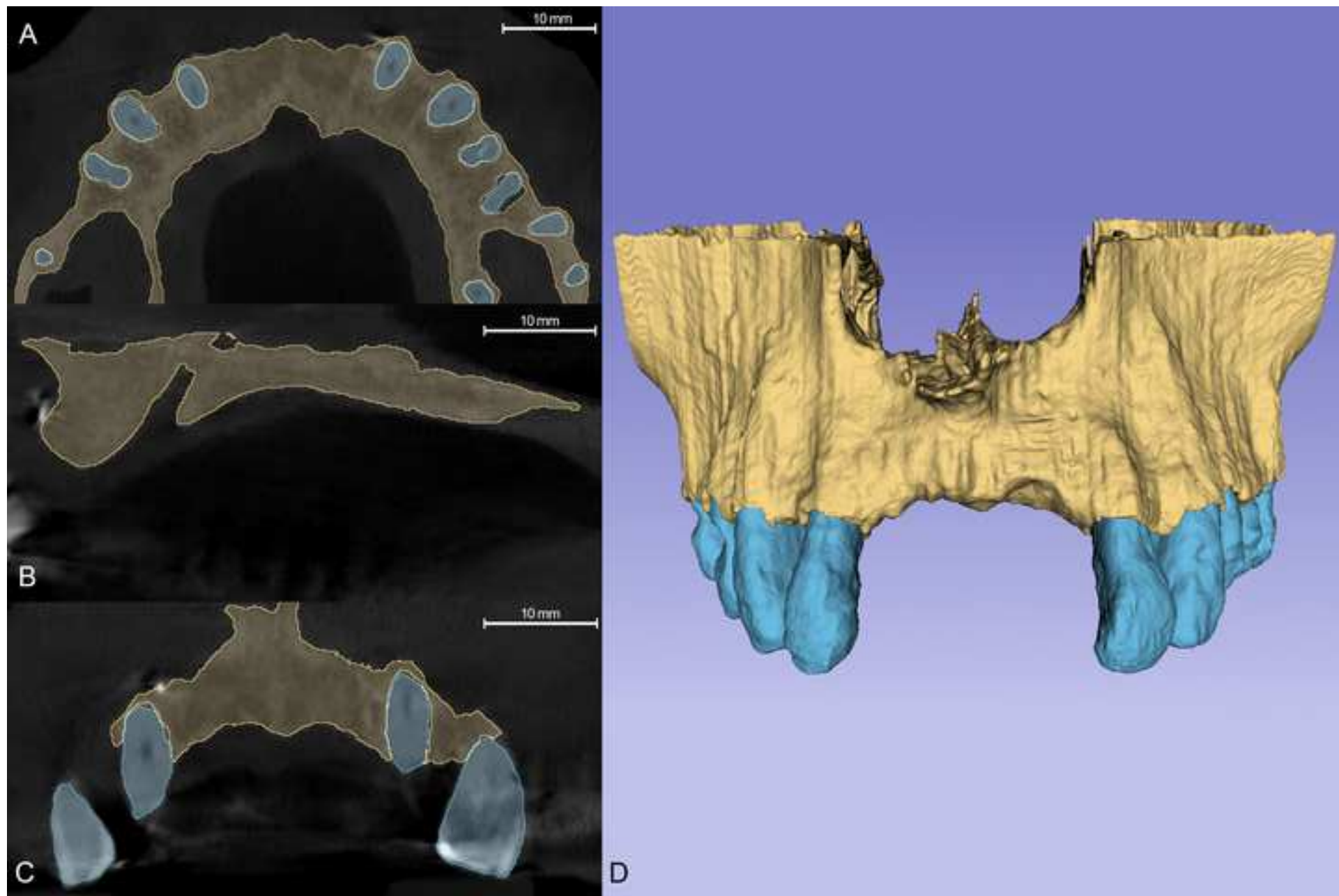
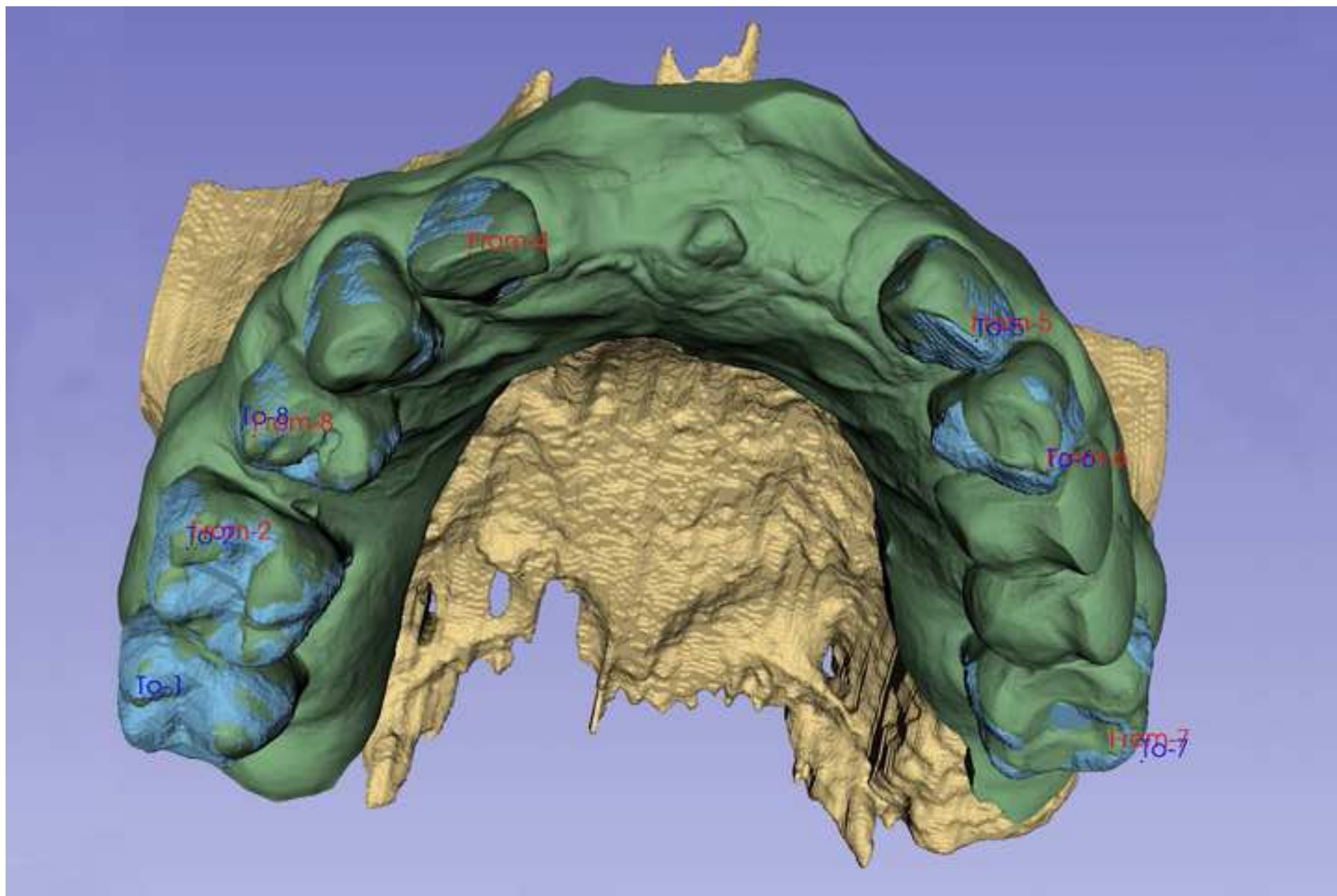


Figure 4

[Click here to access/download;Figure;Figure4.psd](#)





Click here to access/download  
**Video or Animated Figure**  
Animated Figure1.mp4





[Click here to access/download](#)

**Table of Materials**  
**62743\_R2\_Table of Materials.xlsx**



Reply to editorial comments:

Dear Editor, mistakes You pointed out in the manuscript were addressed and corrected to best ability. Thank you for your valuable suggestions.

1. Please take this opportunity to thoroughly proofread the manuscript to ensure that there are no spelling or grammar issues.

Manuscript was previously sent for proofreading; remaining mistakes were corrected.

2. JoVE cannot publish manuscripts containing commercial language. This includes trademark symbols (™), registered symbols (®), and company names before an instrument or reagent. Please remove all commercial language from your manuscript and use generic terms instead. All commercial products should be sufficiently referenced in the Table of Materials. Please sort the Materials Table alphabetically by the name of the material.

Table of materials was sorted

3. Please highlight up to 3 pages of the Protocol (including headings and spacing) that identifies the essential steps of the protocol for the video, i.e., the steps that should be visualized to tell the most cohesive story of the Protocol. Remember that non-highlighted Protocol steps will remain in the manuscript, and therefore will still be available to the reader.

Highlighted areas were revised and changes according to Editors suggestion.

4. Please ensure that the highlighted steps form a cohesive narrative with a logical flow from one highlighted step to the next. Please highlight complete sentences (not parts of sentences). Please ensure that the highlighted part of the step includes at least one action that is written in imperative tense.

Steps were revised carefully one-by-one.

5. Each Figure Legend should include a title and a short description of the data presented in the Figure and relevant symbols.

Figure legends were revised as suggested

6. Please limit the number of Figures to 5 or 6. Please note that we will film the protocol and the presentation of the some the figures may be superfluous.

Number of figures were limited to four plus one animated figure of the finished model.

7. Please add scale bars in the Figures.

Scale bars were added to the images showing 2D views of CBCT datasets, figures showing 3D models are difficult to scale, due to the 2D perspective.

8. Please include an Acknowledgements section, containing any acknowledgments and all funding sources for this work.

“Acknowledgements” and “Funding” sections were added.

9. Please ensure that the references appear as the following: [Lastname, F.I., LastName, F.I., LastName, F.I. Article Title. Source. Volume (Issue), FirstPage – LastPage (YEAR).] For more than 6 authors, list only the first author then et al.

References were revised and edited as suggested

Reply to Reviewer #1:

Dear Reviewer, thank you very much for your positive comments, addition of a face scan is a great idea to improve level of reality. It was added to the manuscript according to Your suggestion.

Reviewer #2:

Dear Reviewer, thank you very much for your positive comments, mistake You pointed out was corrected to: “Utilizing spatial registration of IOS and CBCT data and subsequent free-form surface modelling realistic 3D hybrid models can be acquired visualizing alveolar bone, teeth and soft tissues”

Reviewer #3:

Dear Reviewer, thank you very much for your positive comments, application of virtual planning and execution of navigated surgery in implantology was addressed. Applied voxel size was included in the manuscript.